Int. J. Heat Mass Transfer. Vol. 29, No. 10, pp. 1465–1478, 1986
Printed in Great Britain

0017-9310/86 $3.00+0.00
Pergamon Journals Ltd.

Natural convection on horizontal, inclined, and vertical plates with variable surface temperature or heat flux

T. S. CHEN, H. C. TIEN and B. F. ARMALY

Department of Mechanical and Aerospace Engineering, University of Missouri-Rolla, Rolla, MO 65401, U.S.A.

(*Received* 18 *June* 1985 *and in final form* 11 *February* 1986)

Abstract—An analysis is performed to study the flow and heat transfer characteristics of laminar free convection in boundary layer flows from horizontal, inclined, and vertical flat plates in which the wall temperature $T_w(x)$ or the surface heat flux $q_w(x)$ varies as the power of the axial coordinate in the form $T_w(x) = T_\infty + ax^n$ or $q_w = bx^m$. The governing equations are first cast into a dimensionless form by a nonsimilar transformation and the resulting equations are then solved by a finite-difference scheme. Numerical results for fluids with Prandtl numbers of 0.7 and 7 are presented for three representative exponent values under each of the nonuniform surface heating conditions. It has been found that both the local wall shear stress and the local surface heat transfer rate increase as the angle of inclination from the horizontal γ increases or as the local Grashof number increases. An increase in the value of the exponent n or m enhances the surface heat transfer rate, but it causes a decrease in the wall shear stress. Correlation equations for the local and average Nusselt numbers are obtained for the special cases of uniform wall temperature (UWT) and uniform surface heat flux (UHF). Comparisons are also made of the local Nusselt numbers between the present results and available experimental data for the UHF case, and a good agreement is found to exist between the two.

INTRODUCTION

HEAT TRANSFER by natural convection is frequently encountered in our environment and in engineering devices. Natural convection arises from the buoyancy force induced by density differences in a fluid. Laminar free convection along horizontal, inclined and vertical plates with uniform surface temperature or uniform surface heat flux has been extensively studied analytically (see, e.g. Refs. [1–7]). There are also experimental investigations on natural convection from vertical, inclined, and horizontal surfaces, covering both laminar and turbulent regimes under either a constant-wall-temperature or a constant-surface-heat-flux condition, such as those studies cited in Refs. [8–13]. However, these analytical and experimental studies [1–13] were conducted under the situations of uniform thermal boundary conditions.

In a large number of technical applications, the surface heating conditions are nonuniform and the induced buoyant flow is laminar. This accounts for the fact that laminar free convection with nonuniform surface heatings has also received considerable attention in the past. Sparrow [14] formulated the boundary-layer problem for free convection along a nonuniformly heated vertical flat plate by the Karman–Pohlhausen method and obtained solutions by a series expansion technique. Similarity solutions for free convection on a nonisothermal vertical plate were provided by Sparrow and Gregg [15]. Subsequently, Yang [16] conducted a study of laminar free convection on nonisothermal vertical plates and cylinders to establish various conditions under which a similarity solution exists. A Görtler-type series expansion has also been tried by Kelleher and Yang [17]. Later, Kao *et al.* [18] developed a technique for the solution of free convection on a nonisothermal vertical flat plate by employing local similarity as a first approximation and universal functions for improvement. More recently, Yang *et al.* [19] applied appropriate coordinate transformations and the Merk-type series to solve a similar type of free convection problems. The problem of laminar free convection along a nonisothermal vertical plate with blowing or suction was studied by Huang and Chen [20]. The aforementioned investigations involving nonuniform surface heatings [14–20] are for flow along a vertical flat plate. The problems of free convection on horizontal and inclined flat plates with nonuniform thermal conditions have not received attention. This has motivated the present study.

In the present paper, laminar free convection along horizontal, inclined and vertical flat plates with power-law variation of the wall temperature or with power-law variation of the surface heat flux is analyzed. The boundary layer equations pertinent to this problem contain both effects of streamwise buoyancy force component and buoyancy-induced streamwise pressure gradient in the momentum equations. The governing system of equations is first transformed into a dimensionless form and the resulting equations are then solved by a finite-difference method. Numerical solutions are obtained for fluids having Prandtl numbers of 0.7 (such as air) and 7 (such

NOMENCLATURE

a dimensional constant in the power-law variation of the wall temperature
b dimensional constant in the power-law variation of the surface heat flux
C angle dependent function in equation (67)
D angle dependent function in equation (71)
f, f_1 reduced stream functions defined, respectively, by equations (9) and (18)
F, F_1 reduced stream functions defined, respectively, by equations (27) and (36)
g gravitational acceleration
Gr_x, Gr_L Grashof numbers defined, respectively, as $g\beta[T_w(x)-T_\infty]x^3/\nu^2$ and $g\beta[T_w(L)-T_\infty]L^3/\nu^2$
Gr_x^*, Gr_L^* modified Grashof numbers defined, respectively, as $g\beta q_w(x)x^4/k\nu^2$, and $g\beta q_w(L)L^4/k\nu^2$
h local heat transfer coefficient, $q_w(x)/[T_w(x)-T_\infty]$
$\bar{h}$ average heat transfer coefficient defined by equation (44)
k thermal conductivity
K_1, K_2, K_3, K_4 Prandtl number dependent coefficients defined, respectively, by equations (65), (67), (69) and (71)
L length of plate in the flow direction
m exponent in the power-law variation of the surface heat flux
n exponent in the power-law variation of the wall temperature
Nu_x local Nusselt number, hx/k
$\overline{Nu}$ average Nusselt number, $\bar{h}L/k$
p static pressure difference
Pr Prandtl number, ν/α
q_w local surface heat transfer rate per unit area, $-k(\partial T/\partial y)_{y=0}$
T fluid temperature
u axial velocity component
v normal velocity component
x axial coordinate
y normal coordinate
Y, Y_1 pseudo-similarity variables defined, respectively, by equations (26) and (35).

Greek symbols
α thermal diffusivity
β volumetric coefficient of thermal expansion
γ angle of inclination from the horizontal
ζ, ζ_1 nonsimilar parameters defined, respectively, by equations (31) and (40)
ζ_L, ζ_{1L} nonsimilar parameters defined, respectively, as $(Gr_L^* \cos\gamma/6)^{1/6}\tan\gamma$ and $(Gr_L^* \sin\gamma/5)^{-1/5}\cot\gamma$
η, η_1 pseudo-similarity variables defined, respectively, by equations (8) and (17)
θ, θ_1 dimensionless temperatures defined, respectively, by equations (9) and (18)
Θ, Θ_1 dimensionless temperatures defined, respectively, by equations (27) and (36)
μ dynamic viscosity
ν kinematic viscosity
ξ, ξ_1 nonsimilar parameters defined, respectively, by equations (13) and (22)
ξ_L, ξ_{1L} nonsimilar parameters defined, respectively, as $(Gr_L \cos\gamma/5)^{1/5}\tan\gamma$ and $(Gr_L \sin\gamma/4)^{-1/4}\cot\gamma$
ρ density of fluid
τ_w local wall shear stress, $\mu(\partial u/\partial y)_{y=0}$
ψ stream function.

Subscripts
w condition at the wall
∞ condition at the free stream.

as water) for three representative exponent values of the power-law variation in either the wall temperature or the surface heat flux.

ANALYSIS

Consider a semi-infinite flat plate that is inclined from the horizontal with an acute angle γ and is situated in an otherwise quiescent ambient fluid at temperature T_∞. The x coordinate is measured from the leading edge of the plate and the y coordinate is measured normally from the plate to the fluid. Two surface heating conditions will be considered in the analysis: (1) a power-law variation of the wall temperature, $T_w(x)-T_\infty = ax^n$ and (2) a power-law variation of the surface heat flux, $q_w(x) = bx^m$; where a and b are dimensional constants and m and n are exponents. The gravitational acceleration g is acting downward. For simplicity, the analysis will be presented for the case of fluid above a hot flat surface. This analysis will also be valid for the case of fluid below a cold flat surface.

In the analysis to follow, the fluid properties are assumed to be constant except for the density variation that induces the buoyancy force. With this assumption and the application of the Boussinesq approximation, the governing conservation equations for laminar boundary layer flows can be written as

$$\frac{\partial u}{\partial x}+\frac{\partial v}{\partial y}=0 \quad (1)$$

$$u\frac{\partial u}{\partial x}+v\frac{\partial u}{\partial y}=-\frac{1}{\rho}\frac{\partial p}{\partial x}+g\beta\sin\gamma(T-T_\infty)+v\frac{\partial^2 u}{\partial y^2} \quad (2)$$

$$0=-\frac{1}{\rho}\frac{\partial p}{\partial y}+g\beta\cos\gamma(T-T_\infty) \quad (3)$$

$$u\frac{\partial T}{\partial x}+v\frac{\partial T}{\partial y}=\alpha\frac{\partial^2 T}{\partial y^2}, \quad (4)$$

where the conventional notations are defined in the Nomenclature. It must be pointed out, however, that p is the static pressure difference induced by the buoyancy force (i.e. $p = 0$ outside the boundary layer). The x-momentum and y-momentum equations, equations (2) and (3), can be combined by finding the buoyancy-induced streamwise pressure gradient from equation (3) as

$$-\frac{1}{\rho}\frac{\partial p}{\partial x}=g\beta\cos\gamma\frac{\partial}{\partial x}\int_y^\infty(T-T_\infty)\,\mathrm{d}y. \quad (5)$$

This leads to

$$u\frac{\partial u}{\partial x}+v\frac{\partial u}{\partial y}=g\beta\cos\gamma\frac{\partial}{\partial x}\int_y^\infty(T-T_\infty)\,\mathrm{d}y+g\beta\sin\gamma(T-T_\infty)+v\frac{\partial^2 u}{\partial y^2}. \quad (6)$$

The boundary conditions for the present problem are

$$u=v=0,\quad T=T_w(x)=T_\infty+ax^n \quad \text{or} \quad q_w(x)=bx^m \quad at \quad y=0 \quad (7)$$
$$u\to 0,\quad T\to T_\infty \quad \text{as} \quad t\to\infty.$$

It is noted here that equation (6) reduces to that for a vertical plate without the buoyancy-induced stream pressure gradient term when $\gamma = 90°$ and to that for a horizontal plate without the buoyancy force term when $\gamma = 0°$. The case of uniform wall temperature (UWT) corresponds to $n = 0$, whereas that of uniform surface heat flux (UHF) to $m = 0$.

Next, the system of equations (6), (4) and (7) will be transformed into a dimensionless form, separately for the cases of power-law wall temperature variation, $T_w(x)-T_\infty = ax^n$, and power-law surface heat flux variation $q_w(x) = bx^m$. Owing to the inclination of the plate, the boundary layers are nonsimilar. This point will become clear later.

Power-law variation of wall temperature, $T_w(x)-T_\infty = ax^n$

A. *Horizontal-inclined plate orientation* ($0° \leqslant \gamma < 90°$). Equations (6), (4) and (7) can be transformed from the (x, y) coordinates to the dimensionless coordinates $[\xi(x), \eta(x, y)]$ by introducing

$$\xi=\xi(x),\quad \eta=(y/x)(Gr_x\cos\gamma/5)^{1/5}, \quad (8)$$

where ξ, depending only on x, is the nonsimilar parameter and η is a pseudo-similarity variable. For a similar boundary layer, $\xi = 0$ and η reduces to a true similarity variable. One also introduces a reduced stream function $f(\xi, \eta)$ and a dimensionless temperature $\theta(\xi, \eta)$ defined, respectively, by

$$f(\xi,\eta)=\frac{\psi(x,y)}{5v(Gr_x\cos\gamma/5)^{1/5}},\qquad \theta(\xi,\eta)=\frac{T-T_\infty}{T_w(x)-T_\infty}, \quad (9)$$

in which Gr_x is the local Grashof number and the stream function $\psi(x, y)$ satisfies the continuity equation (1) with $u = \partial\psi/\partial y$ and $v = -\partial\psi/\partial x$.

Substituting equations (8) and (9) into equations (6), (4) and (7), one obtains the following system of equations

$$f'''+(n+3)ff''-(2n+1)f'^2+\xi\theta+\frac{1}{5}\left[(2-n)\eta\theta+(4n+2)\int_\eta^\infty\theta\,\mathrm{d}\eta+(n+3)\xi\int_\eta^\infty\frac{\partial\theta}{\partial\xi}\mathrm{d}\eta\right]=(n+3)\xi\left(f'\frac{\partial f'}{\partial\xi}-f''\frac{\partial f}{\partial\xi}\right) \quad (10)$$

$$\frac{1}{Pr}\theta''+(n+3)f\theta'-5nf'\theta=(n+3)\xi\left(f'\frac{\partial\theta}{\partial\xi}-\theta'\frac{\partial f}{\partial\xi}\right) \quad (11)$$

with the boundary conditions

$$f(\xi,0)=f'(\xi,0)=f'(\xi,\infty)=0;\quad \theta(\xi,0)=1,\quad \theta(\xi,\infty)=0. \quad (12)$$

In the foregoing equations, the primes denote partial differentiations with respect to η, Pr is the Prandtl number, and ξ is found to have the following expression

$$\xi=(Gr_x\cos\gamma/5)^{1/5}\tan\gamma. \quad (13)$$

The physical quantities of interest include the local Nusselt number $Nu_x = hx/k$, the local wall shear stress $\tau_w = \mu(\partial u/\partial y)_{y=0}$, the axial velocity distribution u, and the temperature distribution $\theta(\xi, \eta)$. The first three can be expressed, respectively, by

$$Nu_x=-\theta'(\xi,0)(Gr_x\cos\gamma/5)^{1/5} \quad (14)$$

$$\tau_w=5(\mu v/x^2)(Gr_x\cos\gamma/5)^{3/5}f''(\xi,0) \quad (15)$$

$$ux/v=5(Gr_x\cos\gamma/5)^{2/5}f'(\xi,\eta). \quad (16)$$

It is noted here that the case of uniform wall temperature (UWT) corresponding to $n = 0$ has been treated in Ref. [7]. It is also noted here that the boundary layers become similar and equations (10)–(12) reduce to a system of ordinary differential equations when $\xi = 0$ (i.e. $\gamma = 0°$, the horizontal plate) or when

ξ is a constant, independent of x. The latter situation arises for an inclined plate when $n = -3$.

B. *Vertical-inclined plate orientation* ($0° < \gamma \leqslant 90°$). Equations (10)–(12) become invalid when $\gamma = 90°$ (i.e. for a vertical plate) because for this case $\xi = \infty$. To provide a system of equations that are valid for vertical and inclined plates, with the angle of inclination $(\pi/2-\gamma)$ from the vertical, a separate analysis needs to be performed. To this end, one introduces

$$\xi_1 = \xi_1(x), \quad \eta_1 = (y/x)(Gr_x \sin\gamma/4)^{1/4} \tag{17}$$

and

$$f_1(\xi_1,\eta_1) = \frac{\psi(x,y)}{4\nu(Gr_x \sin\gamma/4)^{1/4}}, \quad \theta_1(\xi_1,\eta_1) = \frac{T-T_\infty}{T_w(x)-T_\infty} \tag{18}$$

in which $\sin\gamma$ arises from $\cos(\pi/2-\gamma)$. The transformation of equations (6), (4) and (7) leads to

$$f_1''' + (n+3)f_1 f_1'' - 2(n+1)f_1'^2 + \theta_1 + \frac{1}{4}\xi_1\left[(1-n)\eta_1\theta_1 + (3n+1)\int_{\eta_1}^{\infty}\theta_1\,d\eta_1 - (n+3)\xi_1\int_{\eta_1}^{\infty}\frac{\partial\theta_1}{\partial\xi_1}d\eta_1\right] = (n+3)\xi_1\left(f_1''\frac{\partial f_1}{\partial\xi_1} - f_1'\frac{\partial f_1'}{\partial\xi_1}\right) \tag{19}$$

$$\frac{1}{Pr}\theta_1'' + (n+3)f_1\theta_1' - 4nf_1'\theta_1 = (n+3)\xi_1 + \left(\theta_1'\frac{\partial f_1}{\partial\xi_1} - f_1'\frac{\partial\theta_1}{\partial\xi_1}\right) \tag{20}$$

$$f_1'(\xi_1,0) = f_1(\xi_1,0) = f_1'(\xi_1,\infty) = 0; \quad \theta_1(\xi_1,0) = 1, \quad \theta_1(\xi_1,\infty) = 0, \tag{21}$$

in which the primes now stand for partial derivatives with respect to η_1. The nonsimilar parameter ξ_1 now has the expression

$$\xi_1 = (Gr_x \sin\gamma/4)^{-1/4}\cot\gamma. \tag{22}$$

The expressions for the local Nusselt number Nu_x, the local wall shear stress τ_w, and the axial velocity distribution can be found as

$$Nu_x = -\theta_1'(\xi_1,0)(Gr_x \sin\gamma/4)^{1/4} \tag{23}$$

$$\tau_w = 4(\mu\nu/x^2)(Gr_x \sin\gamma/4)^{3/4} f_1''(\xi_1,0) \tag{24}$$

$$ux/\nu = 4(Gr_x \sin\gamma/4)^{1/2} f_1'(\xi_1,0). \tag{25}$$

It is noted here that the case of UWT with $n = 0$ has been given in Ref. [5]. In addition, for both an inclined plate with ξ_1 = constant (i.e. $n = -3$) and a vertical plate ($\gamma = 90°$) with $\xi_1 = 0$, equations (19)–(21) reduce to a system of ordinary differential equations. This gives rise to a similar boundary layer problem for both cases.

Finally, through a combination of the above two treatments, free convection of inclined plates for the case of power-law wall temperature variation can be covered for all angles of inclination, $0° \leqslant \gamma \leqslant 90°$.

Power-law variation of surface heat flux, $q_w = bx^m$

A. *Horizontal-inclined plate orientation* ($0° \leqslant \gamma < 90°$). For this case, let

$$\zeta = \zeta(x), \quad Y = (y/x)(Gr_x^* \cos\gamma/6)^{1/6} \tag{26}$$

$$F(\zeta, Y) = \frac{\psi(x,y)}{6\nu(Gr_x^*\cos\gamma/6)^{1/6}}, \quad \Theta(\zeta, Y) = \frac{(T-T_\infty)(Gr_x^*\cos\gamma/6)^{1/6}}{q_w(x)x/k} \tag{27}$$

be, respectively, the dimensionless coordinates, stream function and temperature, where Gr_x^* is the modified Grashof number. Substitution of equations (26) and (27) into equations (6), (4) and (7) yields

$$F''' + (m+4)FF'' - 2(m+1)F'^2 + \zeta\Theta + \frac{1}{6}\left[(2-m)Y\Theta + 4(m+1)\int_Y^{\infty}\Theta\,dY + (m+4)\zeta\int_Y^{\infty}\frac{\partial\Theta}{\partial\zeta}dY\right] = (m+4)\zeta\left(F'\frac{\partial F'}{\partial\zeta} - F''\frac{\partial F}{\partial\zeta}\right) \tag{28}$$

$$\frac{1}{Pr}\Theta'' + (m+4)F\Theta' - (5m+2)F'\Theta = (m+4)\zeta\left(F'\frac{\partial\Theta}{\partial\zeta} + \Theta'\frac{\partial F}{\partial\zeta}\right) \tag{29}$$

$$F(\zeta,0) = F'(\zeta,0) = F'(\zeta,\infty) = 0; \quad \Theta'(\zeta,0) = -1, \quad \Theta(\zeta,\infty) = 0 \tag{30}$$

in which ζ can be found to have the expression

$$\zeta = (Gr_x^*\cos\gamma/6)^{1/6}\tan\gamma \tag{31}$$

and the primes denote partial derivatives with respect to Y.

The local Nusselt number Nu_x, the wall shear stress τ_w, and the axial velocity distribution u are now given respectively by

$$Nu_x = (Gr_x^*\cos\gamma/6)^{1/6}/\Theta(\zeta,0) \tag{32}$$

$$\tau_w = 6(\mu\nu/x^2)(Gr_x^*\cos\gamma/6)^{1/2}F''(\zeta,0) \tag{33}$$

$$ux/\nu = 6(Gr_x^*\cos\gamma/6)^{1/3}F'(\zeta, Y). \tag{34}$$

For both an inclined plate with ζ = constant (i.e. $m = -4$) and a horizontal plate with $\zeta = 0$ (i.e. $\gamma = 0°$) equations (28)–(30) become a system of ordinary differential equations and the boundary layers are thus similar. The case of uniform surface heat flux corresponds to $m = 0$.

B. *Vertical-inclined plate orientation* ($0° < \gamma \leqslant 90°$). When $\gamma = 90°$ (i.e. for a vertical plate), the system of equations (28)–(30) does not hold because ζ becomes infinity. For this reason, a separate analysis is carried out to provide a system of transformed equations for the vertical-inclined orientation.

By introducing for this case

$$\zeta_1 = \zeta_1(x), \quad Y_1 = (y/x)(Gr_x^* \sin\gamma/5)^{1/5} \tag{35}$$

$$F_1(\zeta_1, Y_1) = \frac{\psi(x,y)}{5\nu(Gr_x^* \sin\psi/5)^{1/5}},$$
$$\Theta_1(\zeta_1, Y_1) = \frac{(T-T_\infty)(Gr_x^* \sin\gamma/5)^{1/5}}{q_w(x)x/k}, \tag{36}$$

a transformation of equations (6), (4) and (7) results in

$$F_1''' + (m+4)F_1F_1'' - (2m+3)F_1'^2 + \Theta_1 + \frac{1}{5}\zeta_1$$
$$\times\left[(1-m)Y_1\Theta_1 + (3m+2)\int_{Y_1}^{\infty}\Theta_1\,\mathrm{d}Y_1 - (m+4)\zeta_1\right.$$
$$\left.\times\int_{Y_1}^{\infty}\frac{\partial\Theta_1}{\partial\zeta_1}\mathrm{d}Y_1\right] = (m+4)\zeta_1\left(F_1''\frac{\partial F_1}{\partial\zeta_1} - F_1'\frac{\partial F_1'}{\partial\zeta_1}\right) \tag{37}$$

$$\frac{1}{Pr}\Theta_1'' + (m+4)F_1\Theta_1' - (4m+1)F_1'\Theta_1$$
$$= (m+4)\zeta_1\left(\Theta_1'\frac{\partial F_1}{\partial\zeta_1} - F_1'\frac{\partial\Theta_1}{\partial\zeta_1}\right) \tag{38}$$

$$F_1'(\zeta_1, 0) = F_1(\zeta_1, 0) = F_1'(\zeta_1, \infty) = 0;$$
$$\Theta_1'(\zeta_1, 0) = -1, \quad \Theta_1(\zeta_1, \infty) = 0, \tag{39}$$

in which the primes stand for partial differentiations with respect to Y_1 and the nonsimilar parameter ζ_1 has the expression

$$\zeta_1 = (Gr_x^* \sin\gamma/5)^{-1/5}\cot\gamma. \tag{40}$$

The local Nusselt number, the local wall shear stress, and the axial velocity distribution u are expressible as

$$Nu_x = (Gr_x^* \sin\gamma/5)^{1/5}/\Theta_1(\zeta_1, 0) \tag{41}$$

$$\tau_w = 5(\mu\nu/x^2)(Gr_x^* \sin\gamma/5)^{3/5}F_1''(\zeta_1, 0) \tag{42}$$

$$ux/\nu = 5(Gr_x^* \sin\gamma/5)^{2/5}F_1'(\zeta_1, Y_1). \tag{43}$$

For both a vertical plate ($\gamma = 90°$) with $\zeta_1 = 0$ and an inclined plate with $\zeta_1 = \text{constant}$ (i.e. $m = -4$), equations (37)–(39) reduce to a system of ordinary differential equations and the boundary layers become similar.

A combination of the above two treatments will then cover the entire inclination angles, $0° \leqslant \gamma \leqslant 90°$, for free convection on inclined plates under the power-law variation of surface heat flux.

Average Nusselt numbers

It is of practical interest to determine the average heat transfer coefficient $\bar{h}$ or the average Nusselt number $\overline{Nu}$ for heat transfer calculations. These two quantities are defined, respectively, by

$$\bar{h} = \frac{1}{L}\int_0^L h\,\mathrm{d}x, \quad \overline{Nu} = \frac{\bar{h}L}{k}, \tag{44}$$

where L is the length of plate in the flow direction. The expressions for the average Nusselt numbers are as follows:

A. *For* $T_w(x) - T_\infty = ax^n$

$0° \leqslant \gamma < 90°$

$$\overline{Nu}(Gr_L\cos\gamma/5)^{-1/5} = \frac{5}{n+3}\xi_L^{-1}\int_0^{\xi_L}[-\theta'(\xi, 0)]\,\mathrm{d}\xi \tag{45}$$

$0 < \gamma \leqslant 90°$

$$\overline{Nu}(Gr_L\sin\gamma/4)^{-1/4}$$
$$= -\frac{4}{n+3}\xi_{1L}\int_{\xi_{1x\to 0}}^{\xi_{1L}}\xi_1^{-2}[-\theta_1'(\xi_1, 0)]\,\mathrm{d}\xi_1. \tag{46}$$

In equations (45) and (46), Gr_L, ξ_L, and ξ_{1L} are, respectively, Gr_x, ξ, and ξ_1 evaluated at $x = L$. For $\gamma = 0°$ and $\gamma = 90°$, the corresponding equations are

$$\overline{Nu}(Gr_L/5)^{-1/5} = \frac{5}{n+3}[-\theta'(0)] \tag{47}$$

and

$$\overline{Nu}(Gr_L/4)^{-1/4} = \frac{4}{n+3}[-\theta_1'(0)]. \tag{48}$$

B. *For* $q_w(x) = bx^m$

$0° \leqslant \gamma < 90°$

$$\overline{Nu}(Gr_L^*\cos\gamma/6)^{-1/6} = \frac{6}{m+4}\zeta_L^{-1}\int_0^{\zeta_L}[\Theta(\zeta, 0)]^{-1}\,\mathrm{d}\zeta \tag{49}$$

$0 < \gamma \leqslant 90°$

$$\overline{Nu}(Gr_L^*\sin\gamma/5)^{-1/5}$$
$$= -\frac{5}{m+4}\zeta_{1L}\int_{\xi_{1x\to 0}}^{\zeta_{1L}}\zeta_1^{-2}[\Theta_1(\zeta_1, 0)]^{-1}\,d\zeta_1. \tag{50}$$

The Gr_L^*, ζ_L, and ζ_{1L} in the above equations are, respectively, Gr_x^*, ζ, and ζ_1 evaluated at $x = L$. For $\gamma = 0°$ and $\gamma = 90°$, the corresponding Nusselt number expressions are

$$\overline{Nu}(Gr_L^*/6)^{-1/6} = \frac{6}{m+4}[\Theta(0)]^{-1} \tag{51}$$

$$\overline{Nu}(Gr_L^*/5)^{-1/5} = \frac{5}{m+4}[\Theta_1(0)]^{-1}. \tag{52}$$

Comparison between UWT and UHF cases

The cases of power-law variation of the wall temperature and the surface heat flux can be simplified to the uniform wall temperature (UWT) case when $n = 0$ [3, 5, 7] and to the uniform surface heat flux (UHF) case when $m = 0$. It is of interest to compare the results between UWT and UHF cases. This will be done for the local Nusselt number later when the numerical results are presented.

To facilitate the comparison, one needs to define an equivalent Grashof number for the UHF case in terms of the local wall temperature $T_w(x)$ as

$$(Gr_x)_e = g\beta[T_w(x) - T_\infty]x^3/\nu^2, \quad (53)$$

where

$$T_w(x) - T_\infty = (q_w x/k)(Gr_x^* \cos\gamma/6)^{-1/6}\Theta(\zeta, 0) \quad (54)$$

from equation (27). Substituting equation (54) into equation (53), one obtains

$$(Gr_x)_e \cos\gamma = 6^{1/6}(Gr_x^* \cos\gamma)^{5/6}\Theta(\zeta, 0). \quad (55)$$

With the use of equations (14), (32) and (55), the Nusselt number ratio between the two heating conditions, UWT and UHF, assumes the form

$$\frac{(Nu_x)_{UHF}}{(Nu_x)_{UWT}} = \frac{(5/6)^{1/5}}{[-\theta'(\xi, 0)][\Theta(\zeta, 0)]^{6/5}}. \quad (56)$$

Before the Nusselt number ratio can be determined, the relationship between ξ and ζ needs to be established. From the expressions for ξ and ζ, equations (13) and (31), it can be shown that

$$\xi = (6/5)^{1/5}\zeta[\Theta(\zeta, 0)]^{1/5} \quad (57)$$

under the condition $Gr_x = (Gr_x)_e$.

It is noted that equations (54)–(57) are valid for any angle except $\gamma = 90°$ (i.e. a vertical plate). As for vertical and inclined plates, the following equations for comparisons between the UWT and UHF cases can be obtained in a similar manner:

$$(Gr_x)_e \sin\gamma = 5^{1/5}(Gr_x^* \sin\gamma)^{4/5}\Theta_1(\zeta_1, 0) \quad (58)$$

$$\frac{(Nu_x)_{UHF}}{(Nu_x)_{UWT}} = \frac{(4/5)^{1/4}}{[\Theta_1(\zeta_1, 0)]^{5/4}[-\theta_1'(\xi_1, 0)]}. \quad (59)$$

Here the relationship between ξ_1 and ζ_1 is given by

$$\xi_1 = (4/5)^{1/4}\zeta_1[\Theta_1(\zeta_1, 0)]^{-1/4}. \quad (60)$$

METHOD OF SOLUTION

The system of equations for the power-law variation of wall temperature, equations (10)–(12), and the system of equations for the power-law variation of surface heat flux, equations (28)–(30), both of which are valid for $0° \leqslant \gamma < 90°$, were solved by a finite-difference method modified from that described in Ref. [21]. In this method, the partial differential equations (10)–(12) or (28)–(30) are first reduced to a system of first-order equations which are then expressed in finite-difference form and solved along with their boundary conditions by an iterative scheme. The solutions start with $\xi = 0$ or $\zeta = 0$, which are obtained by a fourth-order Runge–Kutta integration method with a proper step size $\Delta\eta$ or ΔY. With the solutions for $\xi = 0$ or $\zeta = 0$ available for $0 \leqslant \eta \leqslant \eta_\infty$ or $0 \leqslant Y \leqslant Y_\infty$, where η_∞ and Y_∞ are the dimensionless boundary layer thicknesses respectively for the cases of power-law variation of wall temperature and power-law variation of surface heat flux, one proceeds to the first $\xi > 0$ or $\zeta > 0$ location with a proper step size $\Delta\xi$ or $\Delta\zeta$ and obtains a converged solution for the interval $0 \leqslant \eta \leqslant \eta_\infty$ or $0 \leqslant Y \leqslant Y_\infty$ at that ξ or ζ location by iterations, and so on, by marching in the ξ or ζ direction. To conserve space, the details of the numerical solution method are omitted. For the case of $0° < \gamma \leqslant 90°$, solutions were obtained only for vertical plates (i.e. for $\gamma = 90°$) from the system of equations (19)–(21) or (37)–(39) with $\xi_1 = 0$ or $\zeta_1 = 0$ by the Runge–Kutta numerical integration scheme, because the boundary layers for $\gamma = 90°$ are similar. A combination of the two solutions, one for $0° \leqslant \gamma < 90°$ and the other for $\gamma = 90°$, then covers the entire range of inclination angles from horizontal to inclined to vertical for both power-law variations of the wall temperature and of the surface heat flux.

RESULTS AND DISCUSSION

Representative numerical results for both cases of power-law variation of wall temperature and power-law variation of surface heat flux will be illustrated and discussed in this section. The results for the special case of uniform surface heat flux will also be compared with some available experimental data.

Power-law variation of wall temperature, $T_w(x) - T_\infty = ax^n$

The local wall shear stress τ_w in terms of $\tau_w(x^2/5\mu\nu)(Gr_x \cos\gamma/5)^{-3/5}$ and the local Nusselt number Nu_x in terms of $Nu_x(Gr_x \cos\gamma/5)^{-1/5}$ as a function of $\xi = (Gr_x \cos\gamma/5)^{1/5}\tan\gamma$ are shown, respectively, in Figs. 1 and 2 for values of the exponent n of 0, 1/3 and 1, for both $Pr = 0.7$ and 7. As can be seen from the figures, for a given value of n both the wall shear stress and the surface heat transfer rate increase with increasing values of ξ. That is, these two quantities increase with increasing inclination angle γ from the horizontal for a given value of the local Grashof number Gr_x, or with increasing local Grashof number Gr_x for a given inclination angle γ. In addition, the surface

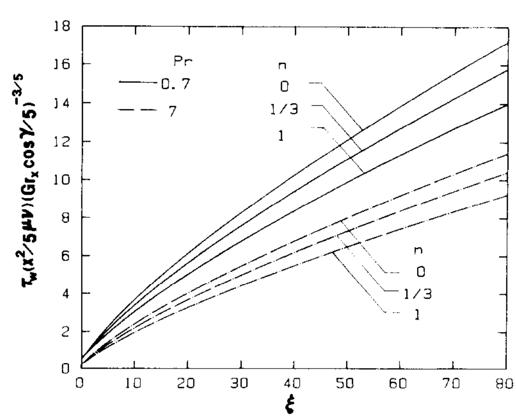

FIG. 1. Local wall shear stress results for the case with $T_w(x) - T_\infty = ax^n$, $Pr = 0.7$ and 7.

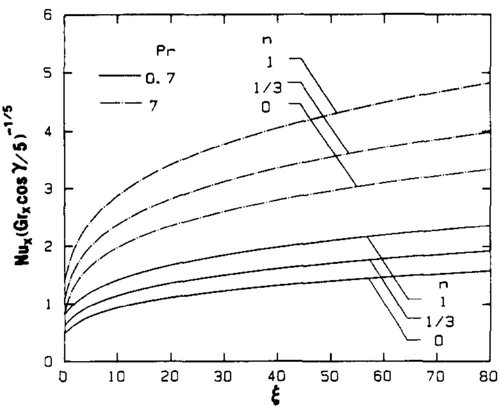

FIG. 2. Local Nusselt number results for the case with $T_w(x)-T_\infty = ax^n$, $Pr = 0.7$ and 7.

heat transfer rate, Fig. 2, is seen to increase with an increase in n for a given value of ξ, with a larger Pr yielding a higher transfer rate. These behaviors can be better illustrated by Figs. 3 and 4 which show, respectively for $Pr = 0.7$ and 7, the variation of the local Nusselt number Nu_x with the local Grashof number Gr_x at various angles of inclination γ for $n = 0$, 1/3 and 1. The curve for $\gamma = 75$ deg. is omitted in both Figs. 3 and 4 because of its closeness to the curve for $\gamma = 90$ deg. (i.e. a vertical plate). These trends are to be expected physically because, for a given n, as the plate is tilted from the horizontal toward the vertical, the buoyancy force becomes more pronounced, and the stronger the buoyancy force the larger will be the wall shear stress and hence the surface heat transfer rate. One may also observe from Figs. 1 and 2 that at a given value of n, while the local wall shear stress is higher for fluids with $Pr = 0.7$ than for fluids with $Pr = 7$, the opposite is true of the local Nusselt number. This trend is due to the fact that a smaller Prandtl number Pr gives rise to a larger velocity gradient at the wall and hence a higher wall shear stress, whereas a larger Prandtl number yields a larger wall temperature gradient and hence a larger heat transfer rate, as can be seen from the representative dimensionless velocity and temperature distributions shown, respectively, in Figs. 5 and 6 for ξ values of 0, 16 and 80.

Inspection of Figs. 5 and 6 also reveals that for a given ξ, the velocity gradient at the wall decreases, whereas the wall temperature gradient increases, as the value of n increases. This fact can help explain the reason why for a given ξ the local wall shear stress decreases as n increases, Fig. 1. A similar behavior

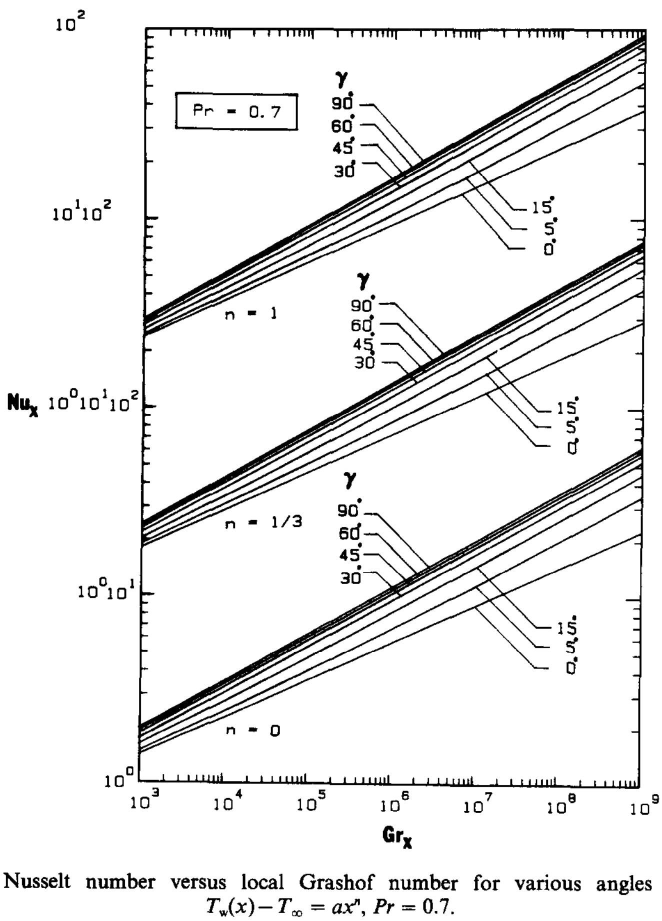

FIG. 3. Local Nusselt number versus local Grashof number for various angles of inclination; $T_w(x)-T_\infty = ax^n$, $Pr = 0.7$.

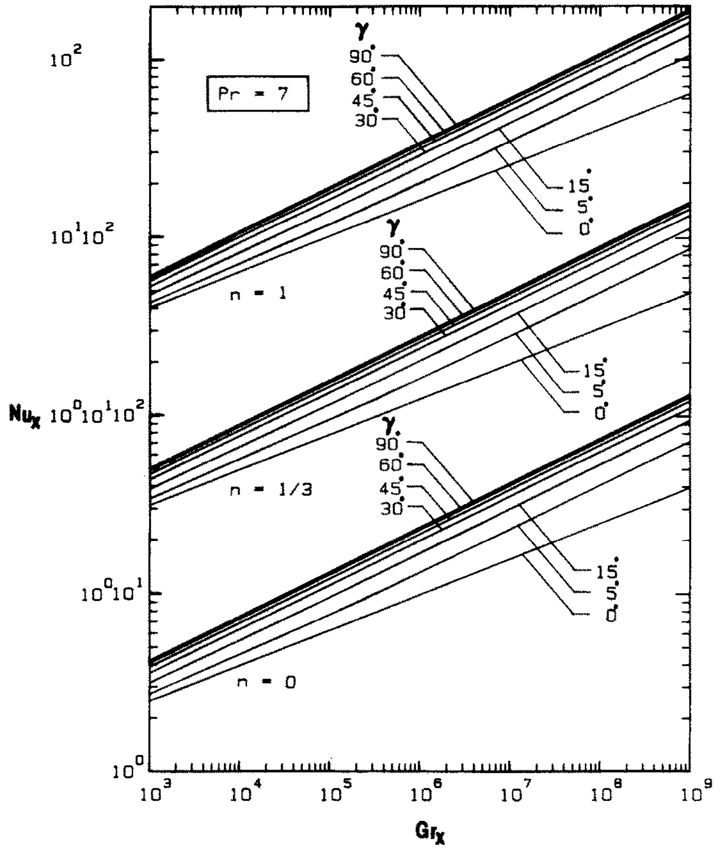

FIG. 4. Local Nusselt number versus local Grashof number for various angles of inclination; $T_w(x)-T_\infty = ax^n$, $Pr = 7$.

has been observed by Sparrow and Gregg [15] in free convection along a nonisothermal vertical plate.

The average Nusselt number results, as calculated from equations (45) and (47), are illustrated in Fig. 7 in terms of $[(n+3)/5]\overline{Nu}(Gr_L \cos\gamma/5)^{-1/5}$ vs ξ_L. As can be seen from the figure, the behavior of the curves is similar to that of the local Nusselt number curves, Fig. 2.

Power-law variation of surface heat flux, $q_w(x) = bx^m$

For this case, the local wall shear stress τ_w in terms of $\tau_w(x^2/6\mu\nu)(Gr_x^* \cos\gamma/6)^{-1/2}$ and the local Nusselt number Nu_x in terms of $Nu_x(Gr_x^* \cos\gamma/6)^{-1/6}$ as a function of $\zeta = (Gr_x^* \cos\gamma/6)^{1/6} \tan\gamma$ are illustrated, respectively, in Figs. 8 and 9 for exponent values of m of -0.4, 0 and 1 and Pr of 0.7 and 7. The variation of Nu_x with Gr_x^* at various angles of inclination γ for

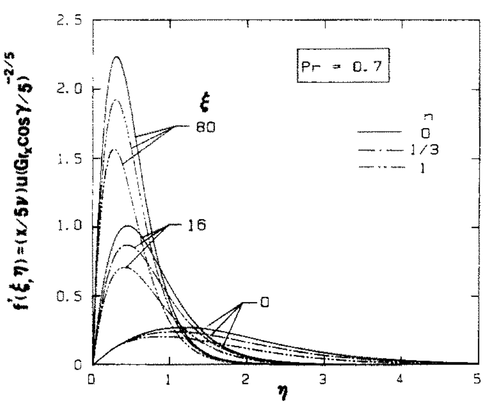

FIG. 5(a). Representative dimensionless velocity distributions at $\xi = 0$, 16, and 80; $T_w(x)-T_\infty = ax^n$, $Pr = 0.7$.

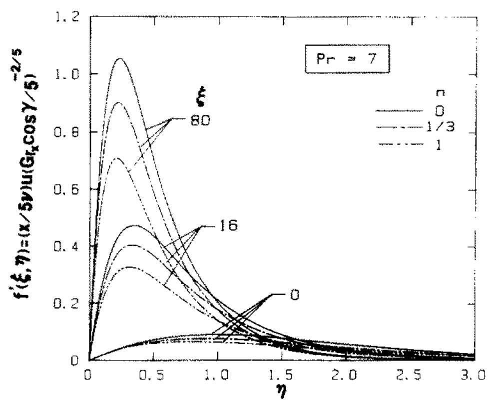

FIG. 5(b). Representative dimensionless velocity distributions at $\xi = 0$, 16, and 80; $T_w(x)-T_\infty = ax^n$, $Pr = 7$.

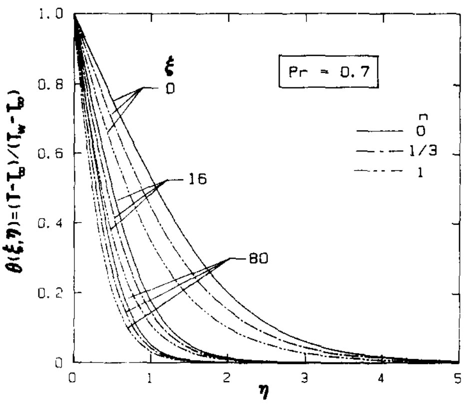

FIG. 6(a). Representative dimensionless temperature distributions at $\xi = 0$, 16, and 80; $T_w(x)-T_\infty = ax^n$, $Pr = 0.7$.

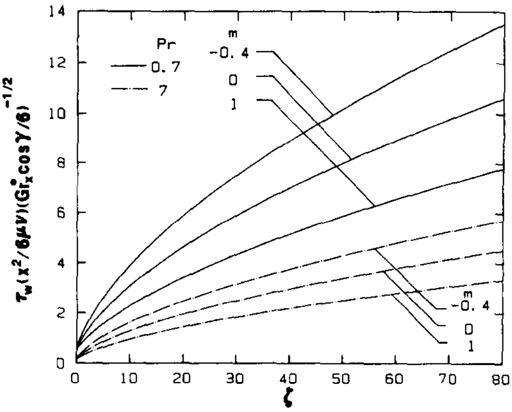

FIG. 8. Local wall shear stress results for the case with $q_w(x) = bx^m$, $Pr = 0.7$ and 7.

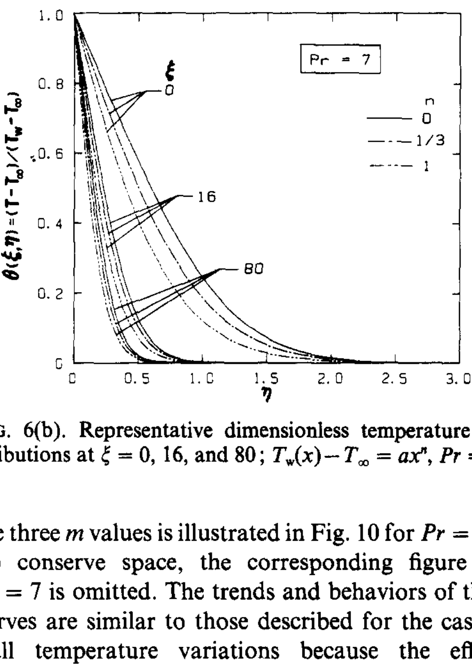

FIG. 6(b). Representative dimensionless temperature distributions at $\xi = 0$, 16, and 80; $T_w(x)-T_\infty = ax^n$, $Pr = 7$.

the three m values is illustrated in Fig. 10 for $Pr = 0.7$. To conserve space, the corresponding figure for $Pr = 7$ is omitted. The trends and behaviors of these curves are similar to those described for the case of wall temperature variations because the effects between the two are similar. Representative velocity and temperature profiles are shown in Figs. 11 and 12, again for $Pr = 0.7$ only, for ζ values of 0, 16 and 80, with m values of -0.4, 0 and 1. It is noted here that the dimensionless temperature is given by $[T(x,y)-T_\infty]/[T_w(x)-T_\infty] = \Theta(\zeta, Y)/\Theta(\zeta, 0)$.

Finally, the average Nusselt numbers evaluated from equations (49) and (51) are shown in Fig. 13. In the figure, the quantity $[(m+4)/6]\overline{Nu}(Gr_L^*\cos\gamma/6)^{-1/6}$ is plotted against ζ_L. Again, the trend of the curves is similar to that of the local Nusselt number curves, Fig. 9.

Comparisons with available experimental results

A thorough comparison of the present numerical results cannot be made with existing work, because no numerical solutions or experimental data for natural convection on inclined plates are available, except for the limiting cases of uniform wall temperature (UWT, $n = 0$) and uniform surface heat flux (UHF, $m = 0$). The local Nusselt number results for the UHF case from the present analysis are compared with the corresponding experimental results of Vliet [10], and Shaukatullah and Gebhart [8] for water in Table 1

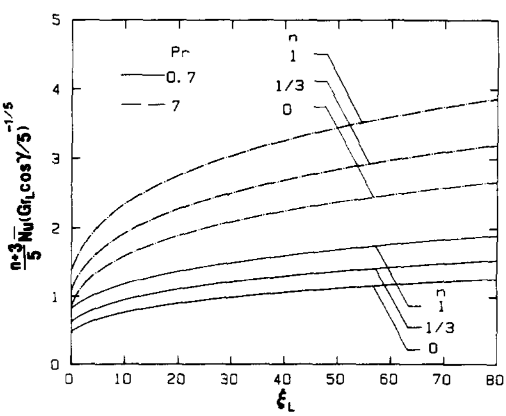

FIG. 7. Average Nusselt number results for the case with $T_w(x)-T_\infty = ax^n$, $Pr = 0.7$ and 7.

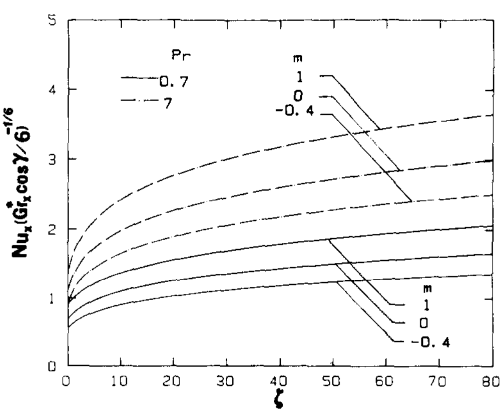

FIG. 9. Local Nusselt number results for the case with $q_w(x) = bx^m$, $Pr = 0.7$ and 7.

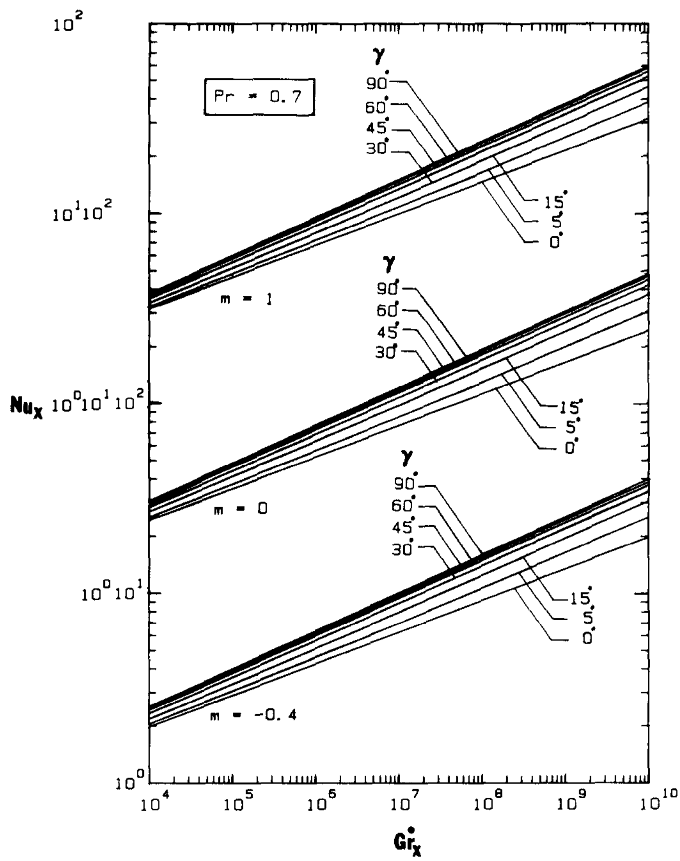

FIG. 10. Local Nusselt number versus modified local Grashof number for various angles of inclination; $q_w(x) = bx^m$, $Pr = 0.7$.

and with those of Vliet and Ross [12] for air in Table 2, for two inclination angles of $\gamma = 30°$ and $75°$. Vliet's results in water [10] give rise to the following correlation equation for the range of inclination angles $30° \leqslant \gamma \leqslant 85°$

$$Nu_x = 0.6(Pr\,Gr_x^*\sin\gamma)^{0.2}. \tag{61}$$

On the other hand, the experimental results of Shaukatullah and Gebhart in water ($Pr = 6$) yield the following correlation equation [8]

$$Nu_x = 0.864(Gr_x^*\sin\gamma)^{0.2}. \tag{62}$$

The results for air obtained by Vliet and Ross have been correlated as [12]

$$Nu_x = 0.55(Pr\,Gr_x^*\sin\gamma)^{0.2}. \tag{63}$$

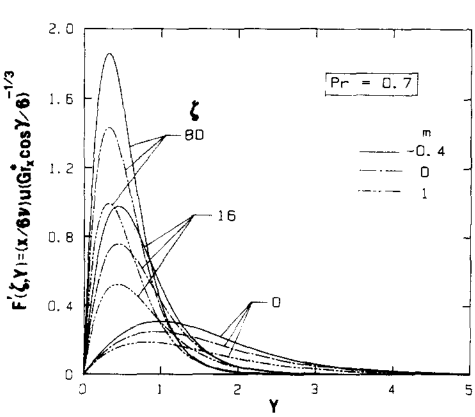

FIG. 11. Representative dimensionless velocity distributions at $\zeta = 0$, 16, and 80; $q_w(x) = bx^m$, $Pr = 0.7$.

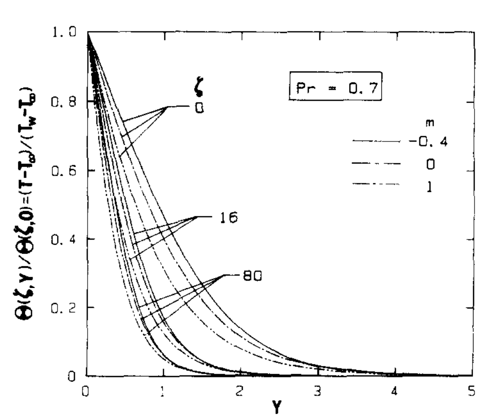

FIG. 12. Representative dimensionless temperature distributions at $\zeta = 0$, 16, and 80; $q_w(x) = bx^m$, $Pr = 0.7$.

Table 1. A comparison between the present results and the experimental results of Vliet [10] and Shaukatullah and Gebhart [8] for free convection to water from inclined plates under a uniform surface heat flux

$\gamma = 30°$				$\gamma = 75°$			
	Nu_x				Nu_x		
Gr_x^*	Present results ($Pr = 7$)	Ref. [10] ($Pr = 7$)	Ref. [8] ($Pr = 6$)	Gr_x^*	Present results ($Pr = 7$)	Ref. [10] ($Pr = 7$)	Ref. [8] ($Pr = 6$)
1.1972×10^4	5.09	5.04	4.92	2.5619×10^4	6.61	6.70	6.53
1.3675×10^5	8.20	8.20	8.00	6.4600×10^4	7.94	8.06	7.86
2.9228×10^6	15.02	15.14	14.77	5.4910×10^5	12.17	12.36	12.06
2.2008×10^7	22.42	22.67	22.12	4.1345×10^6	18.21	18.51	18.06
9.9412×10^7	30.27	30.65	29.91	3.5142×10^7	27.93	28.40	27.71
5.5856×10^8	42.68	43.29	42.24	2.3749×10^8	40.93	41.62	40.61
3.1384×10^9	60.22	61.14	59.66	3.2358×10^9	69.00	70.17	68.47

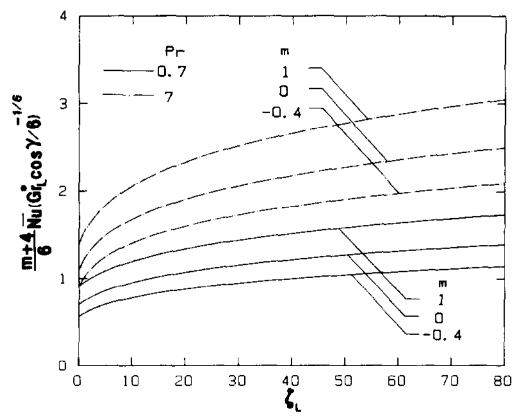

FIG. 13. Average Nusselt number results for the case with $q_w(x) = bx^m$, $Pr = 0.7$ and 7.

As can be seen from Tables 1 and 2, the agreement between the present numerical predictions and the experimental results [8, 10, 12] is very good.

Correlation equations for local and average Nusselt numbers

A. *Local Nusselt numbers.* From the numerical results presented, correlation equations for the local Nusselt numbers, Nu_x, as a function of Pr, Gr_x or Gr_x^*, and γ can be obtained. The correlation equations for the cases of UWT and UHF are listed in the following:

For the UWT case:

$15° \leqslant \gamma \leqslant 90°$

$$Nu_x = K_1(Pr)(Pr\,Gr_x \sin\gamma)^{1/4}, \quad 5 \times 10^3 \leqslant Pr\,Gr_x \sin\gamma \leqslant 5 \times 10^9 \qquad (64)$$

where

$$K_1(Pr) = \frac{3}{4}\left[\frac{2Pr}{5(1+2Pr^{1/2}+2Pr)}\right]^{1/4} \qquad (65)$$

$0° \leqslant \gamma \leqslant 15°$

$$Nu_x = K_2(Pr)(Pr\,Gr_x/5)^{1/5+C(\gamma)}, \quad 10^3 \leqslant Pr\,Gr_x \leqslant 10^9, \qquad (66)$$

where

$$K_2(Pr) = \frac{Pr^{1/2}}{0.25+1.6Pr^{1/2}}, \quad C(\gamma) = 0.070(\sin\gamma)^{1/2}. \qquad (67)$$

Table 2. A comparison between the present results and the experimental results of Vliet and Ross [12] for free convection to air from inclined plates under a uniform surface heat flux

$\gamma = 30°$			$\gamma = 75°$		
	Nu_x			Nu_x	
Gr_x^*	Present results ($Pr = 0.7$)	Ref. [12] ($Pr = 0.7$)	Gr_x^*	Present results ($Pr = 0.7$)	Ref. [12] ($Pr = 0.7$)
1.1972×10^4	2.94	2.92	2.5619×10^4	3.69	3.87
1.3637×10^5	4.67	4.74	6.4600×10^5	4.43	4.66
7.6620×10^5	6.51	6.70	5.4910×10^5	6.78	7.15
2.9228×10^6	8.46	8.76	4.1345×10^6	10.14	10.71
2.2008×10^7	12.57	13.11	3.5142×10^7	15.54	16.43
9.9412×10^7	16.93	17.73	2.3749×10^8	22.75	24.07
5.5856×10^8	23.82	25.04	1.0094×10^9	30.38	32.15
3.1384×10^9	33.57	35.36	3.2358×10^9	38.34	40.59

For the UHF case:

$15^\circ \leqslant \gamma \leqslant 90^\circ$

$$Nu_x = K_3(Pr)(Pr\,Gr_x^*\sin\gamma)^{1/5},\quad 5\times10^4 \leqslant Pr\,Gr_x^*\sin\gamma \leqslant 5\times10^{10}, \tag{68}$$

where

$$K_3(Pr) = [Pr/(4+9Pr^{1/2}+10Pr)]^{1/5} \tag{69}$$

$0^\circ \leqslant \gamma \leqslant 15^\circ$

$$Nu_x = K_4(Pr)(Pr\,Gr_x^*/6)^{1/6+D(\gamma)},\quad 10^4 \leqslant Pr\,Gr_x^* \leqslant 10^{10}, \tag{70}$$

where

$$K_4(Pr) = \frac{Pr^{1/2}}{0.12+1.2Pr^{1/2}},\quad D(\gamma) = 0.038(\sin\gamma)^{1/2}. \tag{71}$$

It is noted here that equations (64) and (68) are modified forms of those given, respectively, in Refs. [22, 23] for the vertical plates in which Gr_x is replaced with $Gr_x\sin\gamma$ and Gr_x^* with $Gr_x^*\sin\gamma$. It has been found that the present numerical results correlate well with equations (64), (66), (68) and (70) within a maximum error of, respectively, 7%, 8%, 7% and 8% for Prandtl numbers of 0.7 and 7. The maximum errors occur at γ near 15° for all correlation equations, as is to be expected.

B. *Average Nusselt numbers*. Next, the correlation equations for the average Nusselt numbers, $\overline{Nu}$, can be derived from the numerical results of equations (45)–(48) and (49)–(52) or by a direct integration of h from equations (64), (66), (68) and (70) to determine $\bar{h}$ and then $\overline{Nu}$ in accordance with equation (44). This latter approach gives rise to the following correlation equations:

For the UWT case:

$15^\circ \leqslant \gamma \leqslant 90^\circ$

$$\overline{Nu} = (4/3)K_1(Pr)(Pr\,Gr_L\sin\gamma)^{1/4},\quad 5\times10^3 \leqslant Pr\,Gr_L\sin\gamma \leqslant 5\times10^9 \tag{72}$$

$0^\circ \leqslant \gamma \leqslant 15^\circ$

$$\overline{Nu} = \frac{K_2(Pr)}{3[1/5+C(\gamma)]}(Pr\,Gr_L/5)^{1/5+C(\gamma)},\quad 10^3 \leqslant Pr\,Gr_L \leqslant 10^9. \tag{73}$$

For the UHF case:

$15^\circ \leqslant \gamma \leqslant 90^\circ$

$$\overline{Nu} = (5/4)K_3(Pr)(Pr\,Gr_L^*\sin\gamma)^{1/5},\quad 5\times10^4 \leqslant Pr\,Gr_L^*\sin\gamma \leqslant 5\times10^{10} \tag{74}$$

$0^\circ \leqslant \gamma \leqslant 15^\circ$

$$\overline{Nu} = \frac{K_4(Pr)}{4[1/6+D(\gamma)]}(Pr\,Gr_L^*/6)^{1/6+D(\gamma)},\quad 10^4 \leqslant Pr\,Gr_L^* \leqslant 10^{10}. \tag{75}$$

In equations (72)–(75), the Prandtl number dependent coefficients $K_1(Pr)$, $K_2(Pr)$, $K_3(Pr)$ and $K_4(Pr)$ and the angle dependent coefficients $C(\gamma)$ and $D(\gamma)$ are as defined by equations (65), (67), (69) and (71). The numerically calculated results from equations (45)–(48) and (49)–(52) correlate well with equations (72), (73), (74) and (75) within a maximum error of, respectively, 10%, 8%, 9% and 5%. Again the maximum errors occur at γ near 15°.

Table 3. Nusselt number ratio $(Nu_x)_{UHF}/(Nu_x)_{UWT}$ for inclined plates, $Pr = 0.7$ and $Pr = 7$

ζ	$Pr = 0.7$: ξ	$Pr = 0.7$: $\frac{(Nu_x)_{UHF}}{(Nu_x)_{UWT}}$	$Pr = 7$: ξ	$Pr = 7$: $\frac{(Nu_x)_{UHF}}{(Nu_x)_{UWT}}$
0	0	1.292	0	1.260
1	1.089	1.226	0.980	1.178
2	2.144	1.197	1.920	1.155
4	4.200	1.172	3.747	1.141
6	6.213	1.162	5.535	1.137
8	8.197	1.156	7.299	1.134
10	10.162	1.153	9.045	1.132
20	19.791	1.147	17.604	1.129
30	29.218	1.145	25.985	1.128
40	38.517	1.144	34.251	1.128
50	47.722	1.143	42.435	1.128
60	56.854	1.143	50.555	1.127
70	65.924	1.143	58.617	1.127
80	74.943	1.142	66.635	1.127
$\infty(\zeta_1 = 0)$	$\infty(\xi_1 = 0)$	1.141	$\infty(\xi_1 = 0)$	1.127

Note: horizontal plates ($\zeta = \xi = 0$); vertical plates ($\zeta_1 = \xi_1 = 0$).

Comparisons of results between UWT and UHF cases

The Nusselt number ratios $(Nu_x)_{UHF}/(Nu_x)_{UWT}$ as a function of ζ or ξ between the UHF and the UWT cases are tabulated in Table 3 for both $Pr = 0.7$ and 7. It is observed from the table that the Nusselt number ratio is always larger than unity, that it decreases with increasing values of ζ (i.e. increasing Gr_x^* for a given γ or increasing γ for a given Gr_x^*), and that the ratio is larger for $Pr = 0.7$ than for $Pr = 7$. In addition, as the plate is tilted from a horizontal to a vertical orientation, the Nusselt number ratio $(Nu_x)_{UHF}/(Nu_x)_{UWT}$ decreases from 1.292 to 1.141 for $Pr = 0.7$ and from 1.260 to 1.127 for $Pr = 7$. A similar comparison of the Nusselt number ratios was performed by Sparrow and Gregg [15] for a vertical plate.

CONCLUSIONS

In this paper, natural convection in laminar boundary layer flows over horizontal, inclined and vertical flat plates has been studied analytically for two surface heating conditions, the power-law variation of the wall temperature and the power-law variation of the surface heat flux. The major findings of the study can be summarized as follows:

(1) Both the local wall shear stress and the local surface heat transfer rate increase with increasing ξ or ζ (i.e. increasing Gr_x or Gr_x^* for a given γ or increasing γ for a given Gr_x or Gr_x^*) for a given value of the exponent n or m and a given Prandtl number Pr.

(2) The local surface heat transfer rate increases with increasing value of the exponent n or m for a given ξ or ζ, but this trend is reversed for the local wall shear stress in terms of $f''(\xi, 0)$ or $F''(\zeta, 0)$.

(3) For a given ξ or ζ and a given exponent n or m, the local surface heat flux increases whereas the local wall shear stress decreases with increasing Prandtl number.

(4) The behavior of the average Nusselt numbers is similar to that of the local Nusselt numbers for all the cases that were investigated.

In addition to the above findings, general correlation equations for the local and average Nusselt numbers that cover various angles of inclination γ and Prandtl numbers (in particular for Pr of 0.7 and 7) are obtained for the special cases of uniform wall temperature (UWT) and uniform surface heat flux (UHF). The correlation equations agree well with calculated numerical results within a maximum error of less than 10%. A comparison between the UHF and UWT cases reveals that the local Nusselt number for the UHF case, $(Nu_x)_{UHF}$, is greater than that for the UWT case, $(Nu_x)_{UWT}$, by some 29 to 14% for a Prandtl number of 0.7 and some 26 to 13% for a Prandtl number of 7. A comparison between the present numerical results and available experimental data for the case of uniform surface heat flux is also made. The agreement between the two is found to be very good.

Acknowledgement—The present study was supported in part by a grant from the National Science Foundation (NSF MEA 83-00785).

REFERENCES

1. S. Ostrach, An analysis of laminar free-convection flow and heat transfer about a flat plate parallel to the direction of the generating body force, *NACA*, TN 2635 (1952).
2. E. M. Sparrow and J. L. Gregg, Laminar free convection from a vertical plate with uniform surface heat flux, *Trans. ASME* **78**, 435–440 (1956).
3. W. T. Kierkus, An analysis of laminar free convection flow and heat transfer about an inclined isothermal plate, *Int. J. Heat Mass Transfer* **11**, 241–253 (1968).
4. L. Pera and B. Gebhart, Natural convection boundary layer flow over horizontal and slightly inclined surfaces, *Int. J. Heat Mass Transfer* **16**, 1131–1146 (1973).
5. M. M. Hasan and R. Eichhorn, Local nonsimilarity solution of free convection flow and heat transfer from an inclined isothermal plate, *J. Heat Transfer* **101**, 642–647 (1979).
6. B. Gebhart, Buoyancy induced fluid motions characteristics of applications in technology—The 1978 Freeman Scholar Lecture, *J. Fluid Engng* **101**, 5–28 (1979).
7. T. S. Chen and K. L. Tzuoo, Vortex instability of free convection flow over horizontal and inclined surfaces, *J. Heat Transfer* **104**, 637–643 (1982).
8. H. Shaukatullah and B. Gebhart, An experimental investigation of natural convection flow on an inclined surface, *Int. J. Heat Mass Transfer* **21**, 1481–1490 (1978).
9. W. W. Yousef, J. D. Tarasuk and W. J. McKeen, Free convection heat transfer from upward-facing isothermal horizontal surfaces, *J. Heat Transfer* **104**, 493–500 (1982).
10. G. C. Vliet, Natural convection local heat transfer on constant-heat-flux inclined surfaces, *J. Heat Transfer* **91**, 511–516 (1969).
11. T. Fujii and H. Imura, Natural-convection heat transfer from a plate with arbitrary inclination, *Int. J. Heat Mass Transfer* **15**, 755–767 (1972).
12. G. C. Vliet and D. C. Ross, Turbulent natural convection on upward and downward facing inclined constant heat flux surfaces, *J. Heat Transfer* **97**, 549–555 (1975).
13. D. L. Siebers, R. J. Moffat and R. G. Schwind, Experimental, variable properties natural convection from a large-vertical, flat surface, *Proc. ASME-JSME Thermal Engng Joint Conf.* **3**, 269–275 (1983).
14. E. M. Sparrow, Laminar free convection on a vertical plate with prescribed nonuniform wall heat flux or prescribed nonuniform wall temperature, *NACA*, TN 3508 (1955).
15. E. M. Sparrow and J. L. Gregg, Similar solutions for free convection from a nonisothermal vertical plate. *Trans. ASME* **80**, 379–386 (1958).
16. K. T. Yang, Possible similarity solutions for laminar free convection on vertical plates and cylinders. *J. Appl. Mech.* **27**, 230–236 (1960).
17. M. Kelleher and K. T. Yang, A Görtler-type series for laminar free convection along a non-isothermal vertical plate, *Q. J. Mech. Appl. Math.* **25**, 447–457 (1972).
18. T. T. Kao, G. A. Domoto and H. G. Elrod, Free convection along a nonisothermal vertical flat plate, *J. Heat Transfer* **99**, 72–78 (1977).
19. J. Yang, D. R. Jeng and K. J. DeWitt, Laminar free convection from a vertical plate with nonuniform surface conditions. *Nume. Heat Transfer* **5**, 165–184 (1982).

20. M. J. Huang and C. K. Chen, Laminar free convection for non-isothermal vertical plate with blowing and suction. *Proc. ASME-JSME Thermal Engng Joint Conf.* **3**, 263–267 (1983).
21. T. Cebeci and P. Bradshaw, *Momentum Transfer in Boundary Layers*, Chapter 7. Hemisphere, Washington (1977).
22. A. J. Ede, Advances in free convection. *Adv. Heat Transfer* **4**, 1–64 (1967).
23. T. Fujii and M. Fujii, The dependence of local Nusselt number on Prandtl number in the case of free convection along a vertical surface with uniform heat flux. *Int. J. Heat Mass Transfer* **19**, 121–122 (1976).

CONVECTION NATURELLE SUR DES PLAQUES HORIZONTALES, INCLINEES OU VERTICALES AVEC DES FLUX DE CHALEUR OU DES TEMPERATURES PARIETAUX VARIABLES

Résumé—On conduit une analyse pour étudier les caractéristiques dynamiques et thermiques des écoulements laminaires de convection naturelle avec couche limite sur des plans horizontaux, inclinés ou verticaux avec une température pariétale $T_w(x)$ ou le flux thermique pariétal $q_w(x)$ varie comme une puissance de l'ordonnée axiale selon $T_w(x) = T_\infty + ax^n$ ou $q_w = bx^m$. Les équations de base sont d'abord mises sous forme adimensionnelle par une transformation de non similitude et les équations résultantes sont ensuite résolues par une méthode de différences finies. Des résultats numériques pour des fluides à nombre de Prandtl entre 0,7 et 7 sont présentés pour trois valeurs d'exposant dans chacune des conditions de surface. On trouve que la tension à la paroi et le taux de transfert thermique augmentent tous les deux quand l'angle d'inclinaison γ à partir de l'horizontale augmente ou quand le nombre de Grashof local croît. L'augmentation de la valeur de l'exposant n ou m favorise le transfert, mais elle cause une diminution de la contrainte pariétale. Des équations sont obtenues pour les nombres de Nusselt locaux et globaux dans les cas spéciaux de température uniforme (UWT) à la paroi et de flux de chaleur uniforme (UHF). Des comparaisons de nombre de Nusselt sont faites pour les cas UHF entre les présents résultats et les données expérimentales et on constate un bon accord entre eux.

NATÜRLICHE KONVEKTION AN HORIZONTALEN, GENEIGTEN UND VERTIKALEN PLATTEN MIT VARIABLER OBERFLÄCHENTEMPERATUR ODER VARIABLER WÄRMESTROMDICHTE

Zusammenfassung—Es wird eine Untersuchung der Strömungs- und Wärmeübergangscharakteristiken bei natürlicher laminarer Konvektion in Grenzschichtströmungen an horizontalen, geneigten und vertikalen ebenen Platten durchgeführt, wobei die Wandtemperatur $T_w(x)$ oder die Oberflächenwärmestromdichte $q_w(x)$ mit der Potenz der axialen Koordinate x in der Form $T_w(x) = T_\infty + ax^n$ oder $q_w = bx^m$ anwächst. Die Erhaltungssätze werden zuerst durch eine nichtkonforme Transformation in dimensionslose Form gebracht, und die so erhaltenen Gleichungen werden mit einem Differenzenverfahren gelöst. Numerische Ergebnisse für Fluide mit Prandtl-Zahlen von 0,7 und 7 werden für drei repräsentative Werte der Exponenten für beide genannten Oberflächenbedingungen vorgelegt. Es zeigte sich, daß sowohl die örtliche Wandschubspannung als auch der örtliche Wärmeübergang mit ansteigendem Neigungswinkel γ von der Horizontalen und mit ansteigender örtlicher Grashofzahl zunehmen. Ein Anstieg in den Werten der Exponenten n oder m erhöht den Wärmeübergang, aber reduziert die Wandschubspannung. Korrelationsgleichungen für die örtlichen und mittleren Nusselt-Zahlen werden für die Spezialfälle der einheitlichen Wandtemperatur (UWT) und der einheitlichen Wärmestromdichte (UHF) ermittelt. Die vorliegenden Ergebnisse für die örtlichen Nusselt-Zahlen werden mit verfügbaren experimentellen Daten für den UHF-Fall verglichen, wobei gute Übereinstimmung festgestellt wird.

ЕСТЕСТВЕННАЯ КОНВЕКЦИЯ НА ГОРИЗОНТАЛЬНЫХ, НАКЛОННЫХ И ВЕРТИКАЛЬНЫХ ПЛАСТИНАХ С ИЗМЕНЯЮЩИМИСЯ ТЕМПЕРАТУРОЙ ПОВЕРХНОСТИ ИЛИ ТЕПЛОВЫМ ПОТОКОМ

Аннотация—Анализируются характеристики ламинарного свободноконвективного течения и теплообмена в режиме пограничного слоя от горизонтальных, наклонных и вертикальных пластин, температура стенки которых $T_w(x)$ или тепловой поток $q_w(x)$ изменяются по степенному закону $T_w(x) = T_\infty + ax^n$ или $q_w = bx^m$. Определяющие уравнения с помощью неавтомодельного преобразования приводятся сначала к безразмерному виду, а затем решаются конечноразностным методом. Численные результаты для жидкостей с числами Прандтля 0,7 и 7 представлены для трех значений показателя степени при каждом из условий неоднородного нагрева поверхности. Найдено, что локальное касательное напряжение на стенке и локальный коэффициент теплообмена на поверхности увеличиваются с ростом угла отклонения от горизонтали γ или локального числа Грасгофа. Увеличение n или m усиливает коэффициент теплообмена на стенке, но уменьшает касательное напряжение на стенке. Корреляции для локального и осредненного чисел Нуссельта получены для случаев однородной температуры стенки и однородного теплового потока на поверхности. Полученные значения локальных чисел Нуссельта сравниваются с имеющимися экспериментальными данными для второго случая, найдено их хорошее соответствие.